Available online at www.sciencedirect.com
ScienceDirect
Polymer 48 (2007) 1729–1740
polymer
www.elsevier.com/locate/polymer

Crystalline morphology of isotactic polypropylene (iPP) in injection molded poly(ethylene terephthalate) (PET)/iPP microfibrillar blends

Gan-Ji Zhong [a], Zhong-Ming Li [a,*], Liang-Bin Li [b,**], Eduardo Mendes [c]

[a] College of Polymer Science and Engineering, State Key Laboratory of Polymer Materials Engineering, Sichuan University, Chengdu, Sichuan 610065, PR China
[b] National Synchrotron Radiation Laboratory and Department of Polymer Science and Engineering, University of Science and Technology of China, Hefei 230026, PR China
[c] Section Nanostructured Materials, Delft University of Technology, Julianalaan 136, 2628 BL Delft, The Netherlands

Received 12 October 2006; received in revised form 23 December 2006; accepted 19 January 2007
Available online 31 January 2007

Abstract

The poly(ethylene terephthalate) (PET)/isotactic polypropylene (iPP) in situ microfibrillar blends have been prepared through a ''slit die extrusion–hot stretch–quenching'' process, in which PET assumes microfibrils with 0.5–15 μm in diameter depending on the hot stretching ratios (HSR, the area of the transverse section of the die to the area of the transverse section of the extrudate). The injection molded specimens of virgin iPP and the PET/iPP blends were prepared by conventional injection molding (CIM) and by shear controlled orientation injection molding (SCORIM), respectively. The effect of shear stress and PET phase with different shape on superstructures and their distribution of injection molded microfibrillar samples were investigated by means of small angle X-ray scattering (SAXS) and wide angle X-ray scattering (WAXS). The shear (or elongational) flow during CIM and SCORIM can induce oriented lamellae (i.e. kebabs induced by shish). The shish-kebab structure appears not only in the skin and intermediated layers of CIM samples, but also in the whole region of SCORIM samples. For the neat iPP samples, a more ''stretched'' shish-kebab structure with higher orientation degree can be obtained in the interior region (intermediate and core layers) by the SCORIM method; moreover, the SCORIM can result in the growth of β-form crystal both in intermediate layer and in core layer, which only appears in intermediate layer of the neat iPP samples obtained by CIM. For the PET/iPP blends, interestingly, the addition of microfibrils as well as their aspect ratios can affect the orientation degree of kebabs only in the intermediate layers, and the addition of microfibrils with a low aspect ratio can bring out a considerable increase in the orientation degree of kebabs along the flow direction. However, for the SCORIM, the addition of microfibrils seems to be a minor effect on the orientation degree of kebabs, and it tends to hamper the formation of a more ''stretched'' shish-kebab structure and suppresses the growth of β-form crystal distinctly. Furthermore, It appears from experiment that γ-form crystals can grow successfully in this oriented iPP melt with the synergistic effect of shear and pressure only when the growth of β crystals can be restrained by some factors, such as the PET dispersed phase and thermal conditions (cooling rate).

Keywords: Crystalline structure; Injection; Shish-kebab structure

1. Introduction

Injection molding is one of the most widely employed methods for manufacturing polymeric products. Nowadays, apart from the academic interest in understanding mechanism leading to different morphologies in an injection molded polymer, the great technological importance of morphology relies on the fact that the polymer characteristics (above all mechanical, but also optical, electrical, transport and chemical) are affected by the morphology (superstructure and its distribution) [1].

The superstructure and its distribution of injection molded semicrystalline polymers are pronouncedly dependent on molding conditions, such as melt temperature, mold temperature, injection speed, mold geometry, etc. [2–7]. In general,

* Corresponding author. Tel./fax: +86 28 8540 5324.
** Corresponding author.
E-mail addresses: zm_li@263.net.cn (Z.-M. Li), lbli@ustc.edu.cn (L.-B. Li).

0032-3861/$ - see front matter © 2007 Elsevier Ltd. All rights reserved.
doi:10.1016/j.polymer.2007.01.056

the melt temperature has a strong effect on the development of skin layer, and its thickness decreases on increasing the melt temperature; however, the studies on influence of other processing conditions, especially stress fields, on its morphologies are still unsatisfactory [3–5]. Additionally, the fiber reinforced semicrystalline polymer composites have currently been widely used, their injection molded parts always present a skin–core structure both in matrix and in fibrillar phase, which leads to the anisotropy of the properties [8–10]. It has been found that the mechanical properties such as strength, stiffness, etc., depend on the aspect ratio of fiber and its distribution as well as fiber orientation distribution [11–13]. However, the relationship between the fibril aspect ratio and the final morphology in injection molded parts, such as skin–core structure, has hardly been studied; little work has focused on the effect of the combination of shear (or elongation) flow and the addition of fibrils with various aspect ratios on the crystalline morphology as well as morphology distribution in injection molded parts, and thorough understanding of the effect of fibril morphology on injection molding induced morphologies and product properties is still not well documented.

In our previous work, the so-called thermoplastic polymer (TP)/TP in situ microfibrillar blends based on thermoplastic engineering polymers (TEP) and polyolefins (PO) mainly polyethylene and polypropylene have been prepared through a ''slit die extrusion–hot stretch–quenching'' process, aiming at developing a simple and convenient approach to property enhancement of commodity polymers and recycling of thermoplastic polymers [14–15]. Significant mechanical reinforcement to the blend was found and the in situ PET microfibrils act as nucleating agents for iPP and PE [16–17]. On the other hand, currently, a novel injection molding, named shear controlled orientation injection molding (SCORIM), has caught particular attention, which imposes dynamic shear stress on polymer melt during cooling, hence leading to a high level of molecular orientation even in the core region. The shear induced crystallization takes place not only in the skin layer but also in the core region until solidification, and the interlocking shish-kebab structure appears in the whole region of the parts [18]; this process can weaken the skin–core structure and improves the mechanical properties effectively [19]. Therefore, using the SCORIM and in situ microfibrillar blends we can investigate in detail the effect of the combination of shear (or elongation) flow and the addition of fibrils on the crystalline morphology as well as morphology distribution in injection molded parts.

In our recent work, for isotactic polypropylene (iPP)/polyethylene terephthalate (PET) microfibrillar blends, the presence of three-dimensional PET microfibrillar network in iPP melt during injection molding leads to polymer parts with homogeneous orientation distribution across the thickness direction. This is of high significance in the processing of semicrystalline polymers, since skin–core structure usually causes anisotropic properties and internal stress. The suppression of the skin–core structure is originated from the re-defined flow field and efficient nucleation of in situ microfiber network. Our results demonstrate that polymer parts with a high and homogeneous orientation can be achieved with a combination of in situ microfibrils and SCORIM method [20]. In the present work, the PET/iPP in situ microfibrillar blends with different hot stretch ratios (HSR, the area of the transverse section of the die to the area of the transverse section of the extrudate) were fabricated by a ''extrusion–hot stretch–quenching'' process, and different shape of PET dispersed phase (sphere and fiber with various aspect ratios) was obtained by controlling HSR. Both CIM and SCORIM were used to prepare the samples. The effect of shear stress and PET dispersed phase with different shape on superstructure and its distribution (i.e. lamellar orientation and its distribution, shish-kebab structure and its distribution, crystalline form and its distribution) of molded microfibrillar blend samples was investigated by means of small angle X-ray scattering (SAXS) and wide angle X-ray scattering (WAXS).

2. Experimental

2.1. Materials

The materials used in this study were poly(ethylene terephthalate) (PET) and isotactic polypropylene (iPP). PET, as the microfibrillar candidate, was a commercial grade of textile polyester and was supplied in pellets by LuoYang Petroleum Chemical Co. (China) with $\overline{M}_n$ about 2.3×10^4 g/mol. Its melt temperature by DSC (differential scanning calorimetry) was ca. 255 °C. The iPP used as the matrix was Model F401, a commercial product of Lanzhou Petroleum Chemical Co. (China) with $\overline{M}_n$ about 11.0×10^4 g/mol and its melt flow index (MFI) was 2.5 g/10 min (190 °C, 21.6 N). In order to avoid hydrolysis, PET was dried in a vacuum oven at 100 °C for at least 12 h prior to processing.

2.2. Preparation of common and in situ microfibrillar PET/iPP blends

The dried PET pellets were dry-mixed with iPP pellets in a fixed weight ratio, 15/85 throughout this study. The extrusion of the mixture obtained was performed on a single-screw extruder having a screw length to screw diameter, *L/D*, of 30. The die for the extruder was a slit die with 35 mm width and 1.0 mm thickness. The temperature profile from the hopper to the die of the extruder was 190, 250, 275, and 270 °C, respectively, and the screw rotation was maintained at 65 rpm. First the extrudate was hot stretched by a take-up device with two pinching rolls to form the microfibrils. The roll temperature was kept at about 40 °C, by adjusting the volume flow rate of tap water in them. Different HSRs could be obtained by changing the speed of the take-up device. In this study, the HSR was set as 1.0, 2.0 and 8.0. The neat iPP also underwent the same procedures only for comparison purposes.

2.3. Preparation of SCORIM and CIM molded samples

The extrudate was pelletized, and then dried for 8 h at 80 °C. The dried pellets were injected into a mold in an

injection molding machine at 200 °C with a injection pressure of 90 MPa. Then, SCORIM technology was applied with a frequency of 0.3 Hz and a pressure of 6 MPa. The mold temperature was about 40 °C. The detailed description of this technology has been reported as follows [19,21,22]. The feature of a melt flow pattern is quite different from that of CIM, and the remarkable difference of the two technologies exists in packing stage, whereas the other stage (i.e. preplasticizing, injection, etc.) is unchanged. The two pistons move out of phase during holding pressure, the shear force would make the iPP melt reciprocatively move in the length direction of moldings, and the shear flow of iPP melt takes place until the gate is solidified (see Fig. 1a). In other words, before being frozen, the iPP melt continuously undergoes repeated shear stress, unless the pistons are stopped. As a result of this, the high shear rate can impose on the melt in interior region with the increase of the thickness of solidified layer. The parts molded by SCORIM have been shown in Fig. 1b. The injection molding was also carried out under static packing (no vibration) under the same processing temperatures. Note that the processing temperature in this stage is far below the melting point of PET (around 255 °C); therefore, the PET microfibrils can be preserved in the injection molded parts [23].

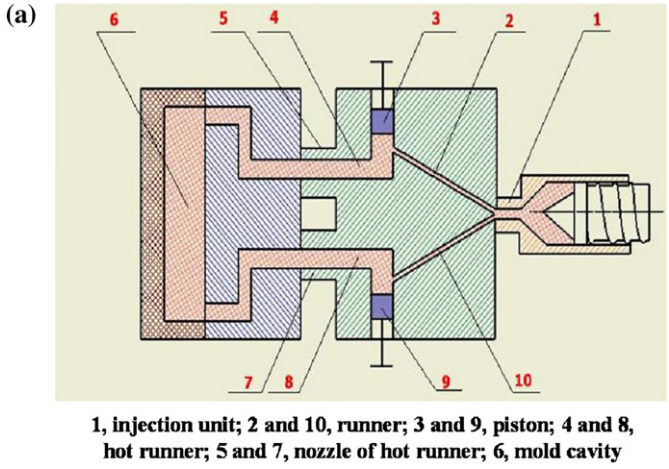

Fig. 1. The schematic of SCORIM (a) and the sketch of part obtained by SCORIM (b).

2.4. Surface morphology observations of PET/iPP blends and iPP SCORIM sample

For phase morphology observation, the matrix iPP in the specimens was selectively dissolved by hot xylene at 110 °C for ca. 1 h. After the solvent volatilized completely, the surfaces were coated with a layer of gold and the domain morphology was observed in a JEOL JSM-5900LV scanning electron microscope (SEM). For the crystalline morphology of iPP, we started with a 6 mm wide and 3.5 mm thick tensile bar and machined away all of the tensile bar except for a 1 mm wide piece (the 3.5 mm thickness remains unchanged) as shown in Fig. 2, and then the polished piece was etched for ca. 36 h in a permanganic reagent – a 7% (w/v) solution of potassium permanganate in an acid mixture consisting of concentrated orthophosphoric acid and concentrated sulfuric acid (2:1, v/v). The surface crystalline morphology of etched sample was observed by atomic force microscopy (AFM). The AFM image was obtained using SPA 400 with SPI 4000 controllers at room temperature.

2.5. The crystal structure and morphology measurement of injection molded samples

To characterize the orientation distribution in thickness direction using X-ray scattering, we also used the sample preparation as shown in Fig. 2. The position of the sample obtained is located in the middle of the bar. The direction normal to MD–TD (the molding direction–transverse direction) plane was defined as ND. The X-ray beam was perpendicular to MD–ND plane and scanned three positions, skin, intermediate and core layers. The skin and intermediate layers are about 100 and 700 μm down from MD–TD surface, respectively. The core layer is in the center of the sample (about 1700 μm down from the MD–TD surface). To characterize the lamellar morphology and its orientation distribution in thickness direction, one-dimensional and two-dimensional SAXS (1D-SAXS, 2D-SAXS) measurements were carried out on a home-built

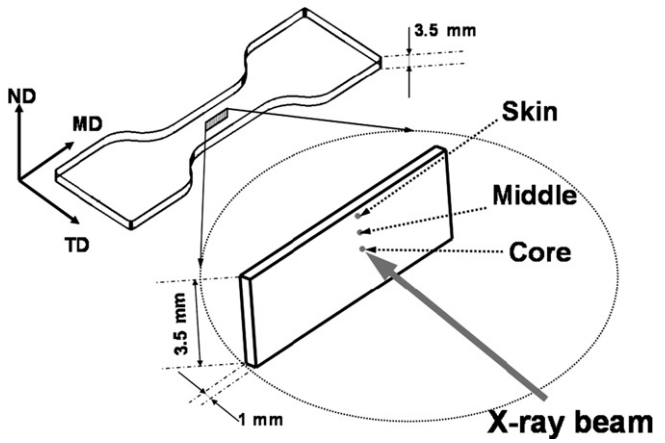

Fig. 2. The schematic of the positions of the sample for X-ray scattering measurement. Key: MD, the molding direction (i.e. flow direction); TD, the transverse direction; ND, the direction normal to the MD–TD plane.

SAXS setup with 18kw Rigaku rotating anode and 2D gas filled detector [24]. To determine the crystalline structure of iPP, one-dimensional WAXS (1D-WAXS) was performed on a Bruker-Nonius D8 Discovery diffractometer with Cu anode operating at 40 kV and 40 mA. The incident X-ray beam is perpendicular to the flow direction. The plane of the specimens used is parallel to the flow direction.

3. Results

3.1. Phase morphology of PET/iPP common and in situ microfibrillar blends

The phase morphology of the PET/iPP (15/85 by weight) blends after undergoing different HSRs is shown in Fig. 3. The common blend (HSR = 1.0) has a typical incompatible blend morphology comprising spherical domains of the minor phase dispersed in iPP matrix (see Fig. 3a). Fig. 3b and c shows that the microfibrillar morphology of the hot xylene-etched surfaces of the as-stretch PET/iPP (15/85 by weight) blends with around 2.0 and 8.0 HSR, respectively. Compared to in situ microfibrillar blend with a higher HSR (i.e. 8.0), the microfibrils in the blend with a lower HSR present a larger size and some ribbon-like morphology particles also appear in the iPP matrix. Additionally, the distribution of microfibrillar diameter becomes narrower and more uniform with the increase of HSR, in good agreement with our previous results [17]. Although the measurement of the aspect ratio is unattainable as it is hard to observe intact microfibrils (see Fig. 3b and c), the SEM images clearly indicate that higher HSR is favorable for the formation of fine microfibrils and responses to the higher aspect ratio.

3.2. The lamellar orientation distribution of iPP in the CIM and SCORIM samples of the microfibrillar blends

Figs. 4 and 5 show the 2D-SAXS patterns at different distances from the surface of the CIM and SCORIM samples, respectively. For the skin layers of the CIM samples, a two-spot pattern in the meridional direction is clearly observed, which indicates the existence of a layer structure, that is, so-called shish-kebab structure [25]. Fig. 6 presents the crystalline morphology near the intermediate layer of SCORIM samples of neat iPP (after the amorphous region was etched away). In this image, the shish-kebab structure can be identified easily. However, these observations are not yet systematic due to the ‘‘immature’’ sample preparation technique.

To determine the lamellar orientation distribution, the orientation parameter of the iPP crystals was estimated using the Hermans orientation parameter, which is defined as

$$\langle P_2(\cos\phi)\rangle = \left(3\langle\cos^2\phi\rangle - 1\right)/2 \quad (1)$$

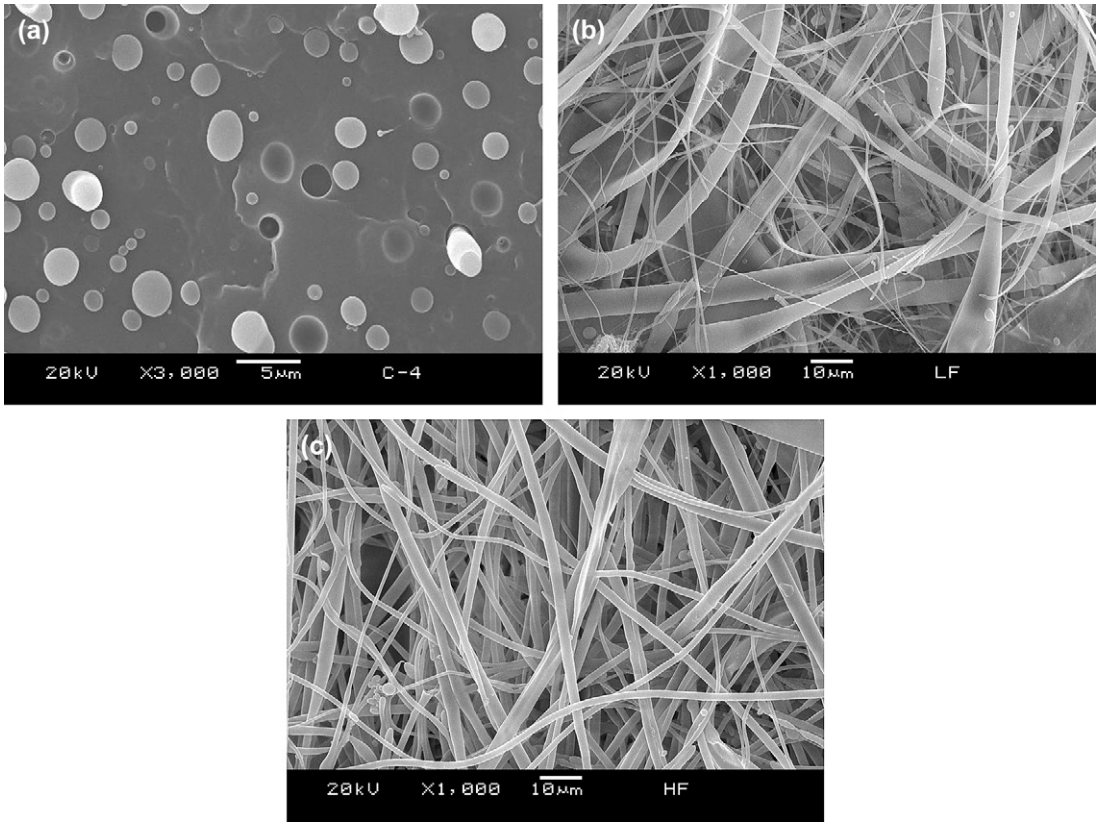

Fig. 3. The SEM morphology of the PET dispersed phase. (a) The cryofractured surface for the common PET/iPP blend (unstretched blend); (b) the microfibrillar PET/iPP blend with low aspect ratio (HSR = 2.0); (c) the microfibrillar PET/iPP blend with high aspect ratio (HSR = 8.0); for the as-stretched sample, the iPP matrix was etched away by hot xylene.

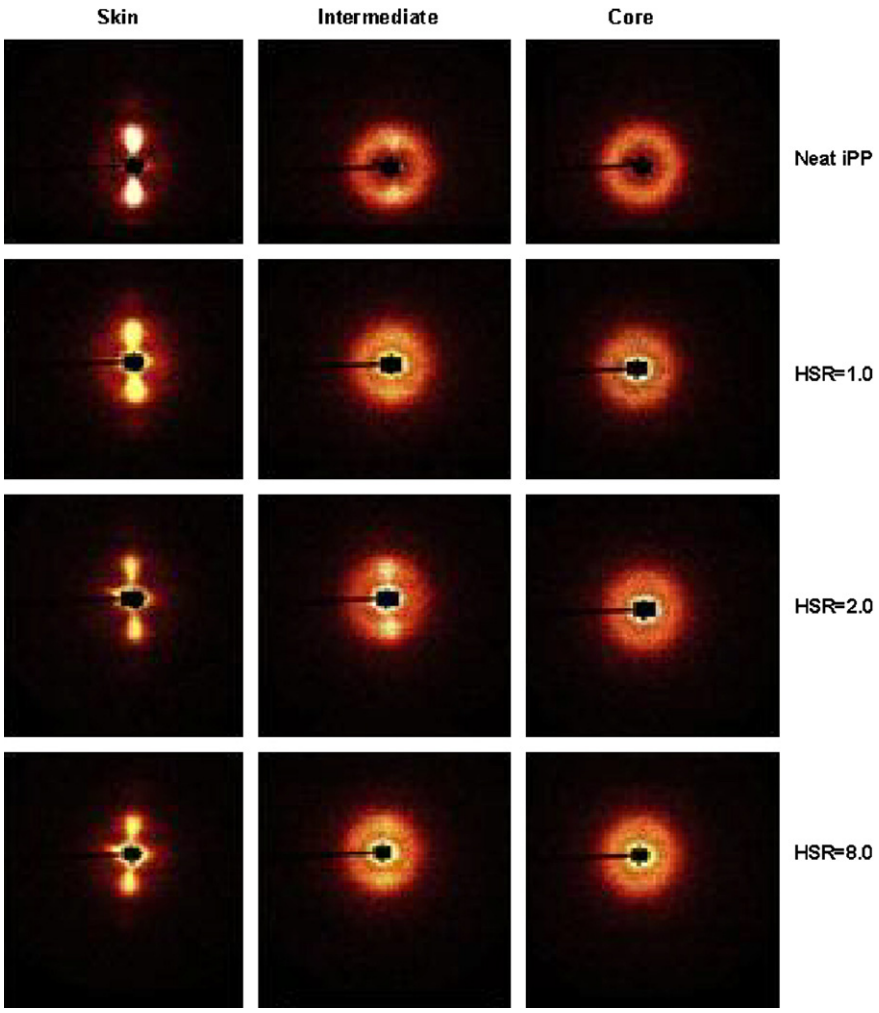

Fig. 4. 2D-SAXS patterns at different distances from the surface of parts obtained by CIM.

where $\langle \cos 2\Phi \rangle$ is an orientation factor defined as

$$\langle \cos^2 \phi \rangle = \int_0^{\pi/2} I(\phi) \cos^2 \phi \sin \phi \, d\phi \Big/ \int_0^{\pi/2} I(\phi) \sin \phi \, d\phi \qquad (2)$$

where $I(\Phi)$ is the scattering intensity at Φ. For our samples, the orientation parameter was calculated mathematically using Picken's method [26]. The orientation parameter has a value of unity when all the lamellae are oriented parallel to the reference direction (i.e. the flow direction in this case), a value of -0.5 when all the lamellae are perpendicular to the reference direction, and a value of zero when there is random orientation in the sample. In our case, the orientation parameter reflects the orientation degree of kebabs along the flow direction, since only kebabs are oriented to the flow direction and can lead to the appearance of scattering maximum in the meridional direction.

Using Eqs. (1) and (2), the lamellar orientation parameters at different distances are calculated from the scattering intensity distribution along the azimuthal angle between 0° and 360°, and are listed in Table 1. For the CIM samples, the orientation parameters have little change with the addition of the PET dispersed phase in the skin layer. In other words, the skin layer for all the CIM samples has almost the same orientation degree of kebabs. In the core regions, the orientation parameters tend to zero, which clearly implies that random orientation is present in the core layers.

Interestingly, for CIM samples, the distinct difference in the orientation parameters exists in the intermediate layers. Compared with the lamellar orientation degree of skin layer, as a whole, the lamellar orientation degrees in this region for all the CIM samples decrease because of the iPP molecular relaxation and relatively low shear stress. But they have a decrease at different levels. The microfibrillar blend with a low aspect ratio has the highest orientation parameter (0.78), followed by the neat iPP (0.56), the microfibrillar blend with a high aspect ratio (0.21) and the common blend (0.06). It suggests that the orientation degree of kebabs in the intermediate layer can be affected by the different shape of PET dispersed phase, and the addition of microfibrils in the blend with a low aspect ratio can bring out a considerable increase in the orientation degree of kebabs along the flow direction.

Upon SCORIM operation, the melt was subjected to shear stress on the packing stage, thus resulting in a distinct increase

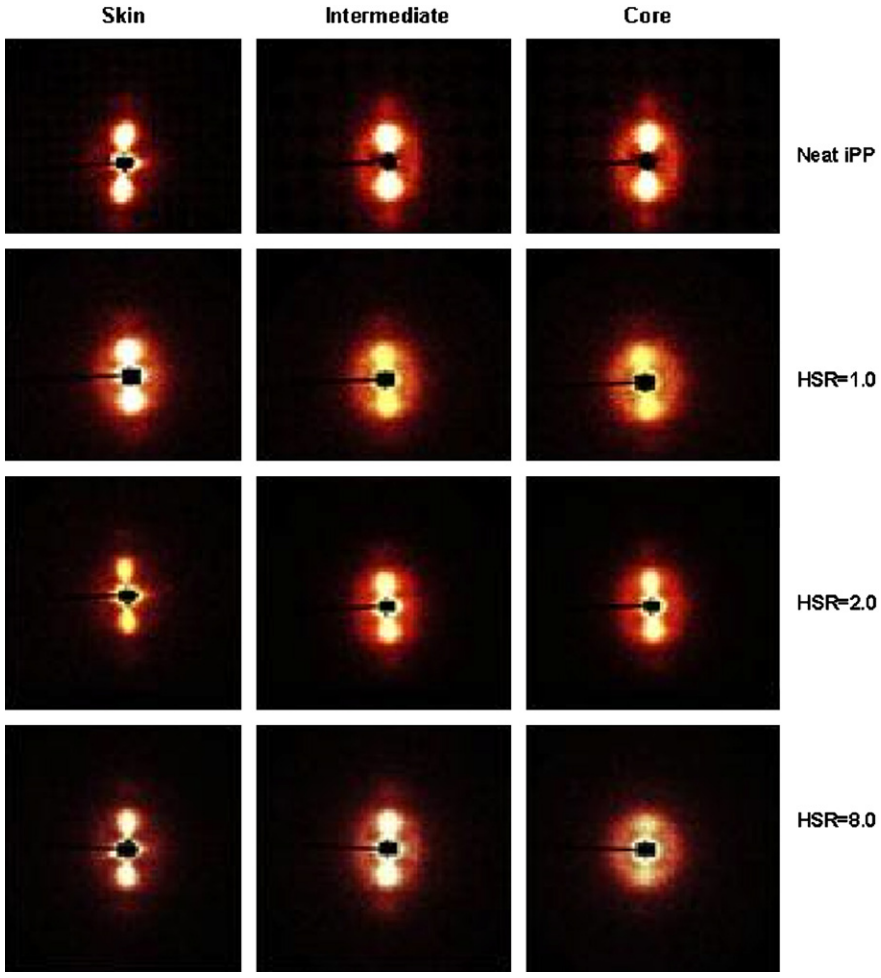

Fig. 5. 2D-SAXS patterns at different distances from the surface of parts obtained by SCORIM.

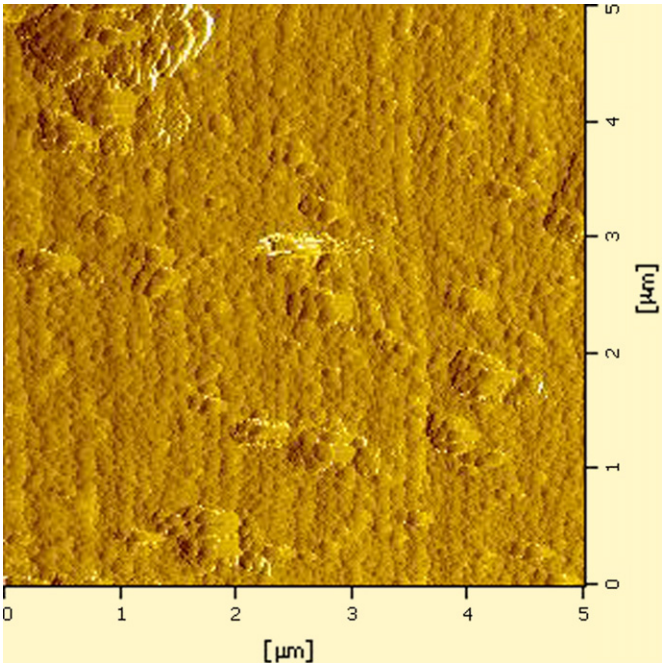

Fig. 6. Atomic force microscopy (AFM) image of the shish-kebab structure in the skin layer of SCORIM molded iPP sample (after the amorphous region was etched away).

of the orientation parameters in intermediate and core layers. Table 1 shows that the orientation parameters in the surface layer are almost keep unchanged, that is, the SCORIM mainly affects the lamellar orientation (kebabs) in the interior region. Compared to the effect of shear force, the existence of the PET dispersed phase with different shape seems to be a minor factor controlling lamellar orientation parameter. Despite this, with the addition of PET dispersed phase, it seems that a more homogeneous orientation degree of kebabs in the thickness direction can be obtained, compared to the neat iPP specimens obtained both by CIM and by SCORIM. As shown in Table 1, the difference of lamellar orientation parameters between skin and intermediate layers for neat iPP (ca. 0.09) is larger than that for blends (ca. 0.02), implying that

Table 1
The orientation parameters at different distances from the surface of parts obtained by CIM and by SCORIM

Samples (CIM)	Skin	Intermediate	Core	Samples (SCORIM)	Skin	Intermediate	Core
Neat iPP	0.90	0.56	0.08	Neat iPP	0.92	0.83	0.86
HSR = 1.0	0.89	0.06	0.09	HSR = 1.0	0.84	0.82	0.80
HSR = 2.0	0.90	0.78	0.04	HSR = 2.0	0.85	0.83	0.83
HSR = 8.0	0.88	0.21	0.05	HSR = 8.0	0.88	0.89	0.88

the orientation degree of kebabs in PET/iPP blends samples is more uniform.

3.3. The long spacing of iPP in the CIM and SCORIM samples of the microfibrillar blends

To probe in more details about the superstructure of iPP in the injection molded samples, the typical 1D-SAXS curves for all the samples in different layers are shown in Fig. 7. One can see a typical scattering density maximum for iPP, which exists in all SAXS curves. Using the Bragg's law ($L = 2\pi/q$), the long period (L) can be estimated from the peak position, as listed in Table 2.

For the CIM samples, the long period does not change considerably except for the skin layer. For the neat iPP, the long period in skin layer is lager than that in the interior region, with the addition of PET phase. The same tendency has been found; however, the level of enhancement in long period decreases, especially, the existence of PET microfibrils with low aspect ratio leads to little difference between the skin layer and interior region. For the SCORIM samples, long period for all samples increases significantly due to the shear stress applied for the melt at the packing stage, especially in

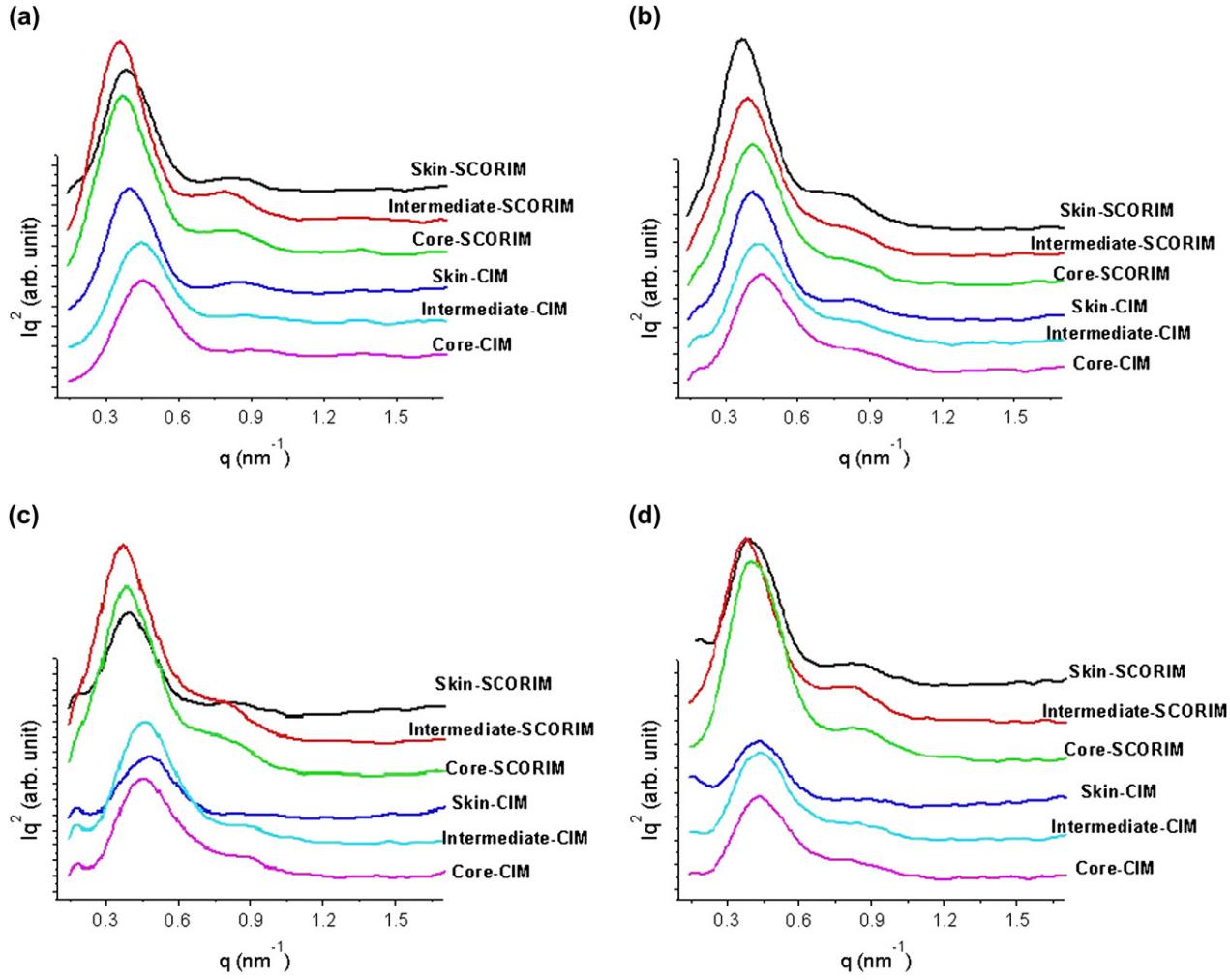

Fig. 7. The one-dimensional SAXS curves at different distances from the surface. (a) The neat iPP; (b) the common PET/iPP blend (unstretched blend, HSR = 1.0); (c) the microfibrillar PET/iPP blend with low aspect ratio (HSR = 2.0); (d) the microfibrillar PET/iPP blend with high aspect ratio (HSR = 8.0).

Table 2
The values of long spacing at different distances from the surface of parts obtained by CIM and by SCORIM

Samples (CIM)	Long spacing (nm)			Samples (SCORIM)	Long spacing (nm)		
	Skin	Intermediate	Core		Skin	Intermediate	Core
Neat iPP	15.3	13.7	13.4	Neat iPP	15.8	17.1	16.3
HSR = 1.0	14.9	13.7	13.6	HSR = 1.0	16.5	15.5	14.7
HSR = 2.0	13.2	13.3	13.1	HSR = 2.0	15.7	16.1	15.6
HSR = 8.0	14.8	13.9	13.8	HSR = 8.0	15.5	16.0	14.9

the interior of the parts. For the blends, the long period in skin layer also increases due to the introduction of SCORIM. It is found that the increase in the long period for neat iPP sample is more marked than that for blend, which reveals that the addition of PET dispersed phase is not beneficial to the increasing of the long period during the crystallization under shear flow. Furthermore, it can be found that the values of long period of the three blends do not have distinct difference. That is, the different shape of PET dispersed phase does not affect the long period of iPP matrix significantly.

3.4. The crystalline form and its distribution of iPP in the CIM and SCORIM samples of the microfibrillar blends

In order to determine crystalline form and its distribution of iPP in CIM and SCORIM samples, the 1D-WAXS measurement was performed at the skin layer, core region as well as intermediate layer (i.e. at about 700 μm from surface). The 1D-WAXS curves for all samples are exhibited in Fig. 8. A Gaussian function was applied to describe the amorphous background. Additional Gaussian functions were inserted, and an iterative peak-fit procedure was used to fit the crystalline reflections of WAXS profiles. The relative fraction of the β-form crystal, K_β, in the crystalline portion of the iPP can be estimated by the Turner–Jones criterion defined as follows [27,28]:

$$K_\beta = \frac{A_\beta(300)}{\sum A_{\text{crystal}}} \tag{3}$$

where $A_\beta(300)$ is the fitted area of the (300) diffraction reflection peak belonging to the β-form crystal. The relative fraction of the β-form crystal at different distances from the surface is shown in Table 3.

For the neat iPP samples, the three layers all exhibit four intense α-form crystal diffraction peaks at 14.1°, 16.9°,

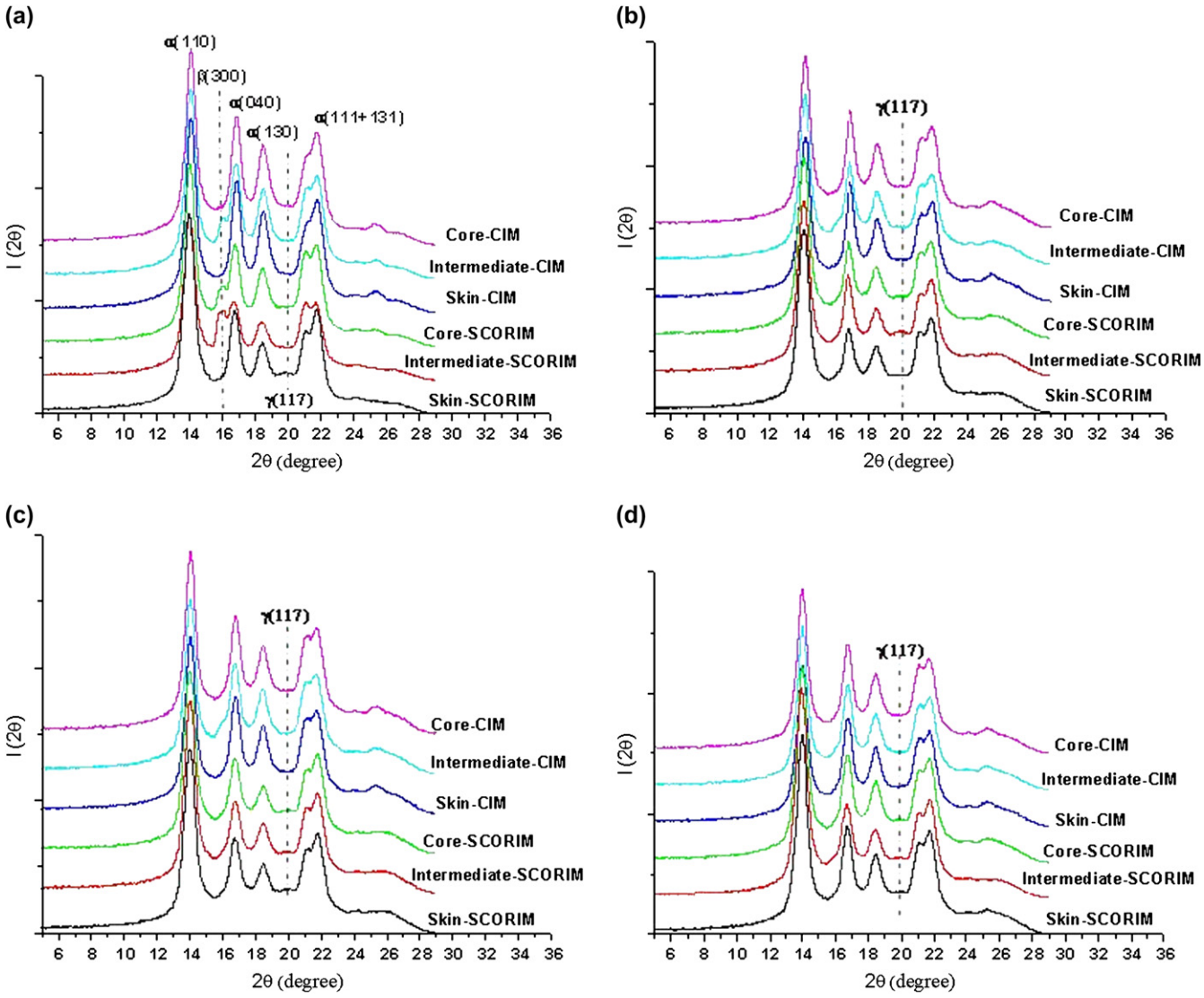

Fig. 8. The one-dimensional WAXS curves at different distances from the surface. (a) The neat iPP; (b) the common PET/iPP blend (unstretched blend, HSR = 1.0); (c) the microfibrillar PET/iPP blend with low aspect ratio (HSR = 2.0); (d) the microfibrillar PET/iPP blend with high aspect ratio (HSR = 8.0).

Table 3
The relative amount of the β-form crystal (K_β) at different distances from the surface in the neat iPP sample

The neat iPP sample	Molded by CIM			Molded by SCORIM		
	Skin	Intermediate	Core	Skin	Intermediate	Core
K_β (%)	0	3.1	0	0	10.0	4.1

18.5° and 21.8° corresponding to (110), (040), (130), and the (111), (131) doublet, respectively (see Fig. 8a) [29]. This reveals that the α-form crystals are dominant in the parts. Moreover, a striking feature of WAXS curve is that the β-form crystals determined by the peak at $2\theta = 16.1°$ also appear in the intermediate layer of the CIM samples, whose relative concentration (K_β) is around 3.0% (see Table 3). Furthermore, for SCORIM iPP parts, the K_β in the intermediate layer increases distinctly (ca. 10.0%) and the β-form crystals also appear in the core region (K_β is around 4.0%). It should be noted that the β-form crystals are not detected by WAXS in the skin layer of all samples although the melted iPP in this layer suffers strong shear (or elongate) stress. As for the PET/iPP blends, the 1D-WAXS did not detect any β-form crystals. It indicates that the addition of PET dispersed phase hinders the formation of β-form crystals apparently, regardless of the shape of dispersed phase.

In addition to the α- and β-form crystals, there are also a small amount of γ-form crystals formed in skin layer of the SCORIM iPP samples, which can be identified by the γ reflection (117) corresponding to $2\theta = 20.05°$ [30]. For SCORIM PET/iPP blend, the γ reflections were detected not only in skin layer but also in the interior region (intermediate and core layers). Note that the interior region of SCORIM iPP sample does not exhibit distinct γ reflection (117) but exhibits β reflection (300) as shown in Fig. 8a. Therefore, it seems to suggest that the growth of γ-form crystals could be restrained by growth of β-form crystals. For the three CIM blend samples, it is hard to obtain the γ-form crystals.

4. Discussions

4.1. The effect of SCORIM technology on the crystalline structure of iPP

For simplicity, we just take into account the neat iPP samples in this section; the PET/iPP blend will be considered in the next section. For the CIM iPP sample, according to the bimodal structure in the injection molded parts [25], the skin layer is composed of shish-kebab main skeleton structure, whose axis is parallel to molding direction (MD), pile epitaxially with *a**-axis-oriented imperfect lamellar substructure (see Fig. 9). The shish and *a**-axis-oriented lamellae must lead to the appearance of scattering maximum on the equator of SAXS patterns. However, this scattering was not observed (see Figs. 3 and 4). Fujiyama and Wakino [25] attributed the disappearance of this scattering to the lesser perfection of the *a**-axis oriented lamellae. Moreover, in the core regions, the orientation parameters tend to zero (see Table 1, core layer

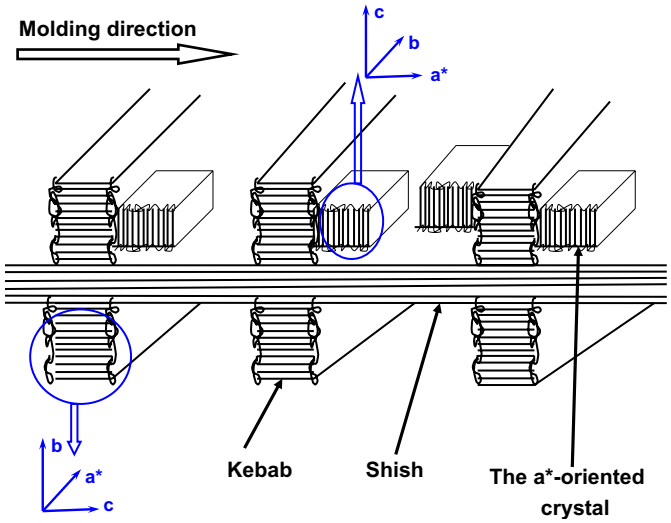

Fig. 9. The schematic of the shish-kebab structure as well as the *a**-orientation crystallization [25,28].

of CIM samples), which seems to infer that the kebabs do not appear in the core layers. In contrast, from the 2D-WAXS measurements [20], the degree of iPP molecules for PET/iPP microfibrillar blend is around 0.21 in the core region, indicating that the row nuclei induced crystallization has taken place and kebabs must exhibit in this region. This is probably a consequence of small size and less perfection of shish-kebab structure existing in the core region and the SAXS cannot detect this layer-like structure, because the relaxation of oriented iPP molecules inevitably occurs due to a low cooling rate in the core region. Unfortunately, the assumption mentioned above is lacking of direct experimental evidence of the size and perfection of shish-kebab structure, and further investigations on that will be carried out in future work.

Based on the flow profile of SCORIM mentioned in Section 2, we can discuss the effect of SCORIM on the superstructure of samples. The reciprocating movement of pistons brings out disentanglement of iPP polymer chains, which tend to orient in the molding direction (flow direction) not only in the skin layer but also in the interior region (including intermediate and core layers). The oriented iPP melt will form row nuclei (or shish) at high onset temperatures (ca. 150 °C) [31,32]. Then, kebabs can grow epitaxially on shish, and subsequently, the shish-kebab structure along the flow direction forms both in skin layer and in interior region. This is attributed to the noticeable increase of lamellar orientation degree (i.e. the orientation degree of kebabs) (see Table 1, SCORIM samples).

Compared to that of CIM iPP, the amount and size of row nuclei (or shish) would be enhanced apparently by the reciprocating shear stress in the intermediate and core layer [33], and then a more ‘‘stretched’’ shish-kebab structure can form and that, in turn, gives rise to an overall increase in the average long spacing. That is, a more ‘‘stretched’’ shish-kebab structure in the interior region by the SCORIM may attribute to the distinct increase of long spacing of iPP, especially in intermediate layer and core region (see Table 2). In addition, the long spacing of iPP in intermediate layer is longer than that

in core region, indicating that shear rate exhibits a maximum near the intermediate layer leading to more distinct shish-kebab structure. It should be pointed out that this shear stress has little influence on lamellar orientation and long spacing of iPP in skin layer (see Tables 1 and 2), which can be explained as follows: (1) the degree of lamellar orientation is also high in CIM samples due to the enlongational flow; (2) the flow profile of iPP melt in skin layer is the same as that of CIM (enlongational flow) at the filling stage of SCORIM, then the reciprocating shear stress is imposed on the iPP melt of skin layer; however, it is hard to increase the degree of lamellar orientation any more by this low shear rate (ca. $10\ s^{-1}$) calculated by the mold geometry due to rapid cooling near the cavity wall.

With regard to the three-form crystals coexisting in samples, it was shown in some other researchers' work that point-like spherulitic nuclei on shear induced row nuclei may induce an α to β modification transition only when the kinetic prerequisite G_β (the growth rate of the β crystals of iPP) $> G_\alpha$ (the growth rate of α crystals of iPP) is fulfilled [34,35]. Furthermore, it was demonstrated unambiguously that iPP crystallization between $T_{\alpha\beta}$ (ca. 140 °C) and $T_{\beta\alpha}$ (ca. 105 °C) hold this kinetic prerequisite [34]. Based on these facts, we can explain the origin of β crystals and their distribution in our case as follows: When the SCORIM method was applied, the shish-kebab structure appeared in the three regions (see Fig. 5), which indicates that the row nuclei can form in the whole region. That is, the β crystals can grow on them as long as the crystalline temperature for iPP holds the aforementioned kinetic prerequisite. However, the crystallization time for iPP between $T_{\alpha\beta}$ and $T_{\beta\alpha}$, which is defined as t_β, is too short to form a certain amount of row nuclei induced β crystals in the skin layer that can be detected by WAXS due to the large cooling rate. Consequently, the (040) reflection of β crystals has not been observed both in skin layer of SCORIM iPP sample and in that of CIM iPP sample (see Fig. 8a, skin-CIM and skin-SCORIM). On the contrary, the cooling rate is relatively slow in interior region (intermediate and core layers) due to bad heat conduction of skin layer; as a result, the t_β is long enough to form a certain amount of β crystals that WAXS can detect (see Fig. 8a, intermediate-SCORIM, core-SCORIM and intermediate-CIM). Moreover, the amount of β crystals in intermediate layer of SCORIM sample is more than that in core layer (see Table 3), which attributes to a relatively higher amount and lager size of row nuclei (or shish) in intermediate layer as discussed above. That is, the shear rate displays a maximum near the intermediate layer as deduced by the data of long spacing of iPP. As for core layer of CIM iPP sample, it should be noted that the level of shear is very low and it is hard to form many row nuclei on which the β crystals can grow (see Fig. 8a, core-CIM).

4.2. The effect of the PET phase on the crystalline structure of iPP

The effect of the PET dispersed phase as well as its shape on the iPP superstructure of injection molded parts are considerably complex. In our previous studies on the PET/iPP blend, it is found that the influence of microfibrillar network on iPP molecular orientation has two opposite effects: (1) shear induced and fibril-assistant induced orientation. The existence of PET dispersed phase can enhance the onset of crystallization temperature and reduces the half time of crystallization of iPP under quiescent condition [17]. Furthermore, the row nuclei can be induced both by PET fibril and by simple shear rate under shear flow [32,36], and the crystallization rate and the onset of crystallization temperature can be improved further. This phenomenon is favorable to the preservation of oriented iPP molecules. (2) The PET microfibrils lessen the flow ability of iPP melt. At the same injection pressure, compared to the neat iPP, the iPP melt containing PET microfibrillar network or PET sphere-like particle has a lower flow rate to fill the mold due to higher viscosity [37], which causes the weakness of iPP molecules' movability as well as the level of molecular orientation.

With regard to the degree of lamellar orientation, it is a balance between the two factors. For the CIM, the little difference of lamellar orientation degree in skin layers indicates that the elongational flow can induce shish-kebab structure along the flow direction so severe as to cover the effect of PET dispersed phase. Moreover, the larger cooling rate near the wall can suppress the relaxation of shish effectively. The shear flow appears between the solidified skin layers and induces the alignment of iPP molecules along the flow direction during the filling stage. For each sample, the degree of lamellar orientation in the interior region (intermediate and core layers) is less than that in skin layer (see Table 1), since the shear flow is less effective to induce orientation than elongational flow [38]. Upon the cessation of the flow, the oriented iPP molecules begin to relax; therefore, the ultimate degree of lamellar orientation is a balance between the flow induced orientation and relaxation of oriented segments. From Table 1 (the CIM samples), the latter factor is dominant in common PET/iPP blend and PET/iPP microfibrillar blend with a high aspect ratio, whereas the former factor is dominant in PET/iPP microfibrillar blend with a low aspect ratio. The reason for this phenomenon has not been understood yet at present. For SCORIM, there is nearly no difference between the lamellar orientation degree of neat iPP and that of PET/iPP blend, implying that the oscillation shear force becomes a dominant factor and the positive influence of the PET dispersed phase on the orientation degree of shish-kebab structure (the former factor) can compensate for the negative one. Moreover, as discussed in earlier publication [20], micro-channels or pores were formed by the microfibrillar network of PET, which acted as stir to define and homogenize the flow field in iPP melt across the thickness direction and consequently the orientation of crystals. All the facts are suggested to be contributors for the little difference of the degrees of lamellar orientation in the three locations of all the samples.

As for long period of iPP, one can deduce that the PET dispersed phase has little influence on the long period in interior region (see Table 2, CIM samples, intermediate and core layers) where the shear rate is very low, that is, the

heterogeneous nucleation of PET dispersed phase cannot affect the long spacing of lamellar stacks for bulk iPP for all samples, which is constant with our earlier publication [17]. Note that the amount and size of shish-kebab structure are not enough to cause the increase of long spacing of iPP since the kebabs indeed exist in intermediate layer of CIM samples (see Fig. 3). Under the higher flow (shear or elongation) field (i.e. skin layer of CIM sample, the whole region in SCROIM samples), the addition of PET dispersed phase can cause a decrease in the long spacing of iPP, compared with the SCORIM iPP sample. The phenomenon can be attributed to the latter factor mentioned above. The size of the more "stretched" shish-kebab structure decreases due to relatively low shear rate, which may attribute to less increase of long spacing of iPP, compared to the CIM iPP sample. Additionally, the weak effect of PET phase on the long period happening in skin layer may be due to the higher cooling rate near the wall. On the one hand, the higher cooling rate is favorable to the retention of orientation; on the other hand, the higher cooling rate leads to shorten the time imposed on the iPP melt during the SCORIM process, which tends to decrease the level of lamellar orientation.

It was shown by WAXS that the addition of PET dispersed phase hampered the formation of β crystals. The similar results have been reported by Saujanya and Radhakrishnan [39], and they did not find the β crystals in PET fibril filled iPP composite. The phenomenon may be ascribed to the heterogeneous nucleation of PET dispersed phase. The existence of PET dispersed phase can enhance the onset crystallization temperature by 10 °C (at ca. 130 °C) and reduces the half-crystallization time under quiescent condition [17]. The values of these two crystallization parameters can increase further under shear field due to shear induced crystallization [32]; whereas only the iPP crystallization between $T_{\alpha\beta}$ (ca. 140 °C) and $T_{\beta\alpha}$ (ca. 105 °C) facilitates the formation of β crystals. Therefore, the PET phase leads to iPP crystallization at higher temperature, which is not favorable to form a considerable amount of β crystals that can be detected by WAXS. Furthermore, the different shape of PET dispersed phase has little influence on the formation of β crystals in our case. Interestingly, the addition of PET dispersed phase is favorable to the formation of γ-form crystals in SCORIM. The γ-form is known to grow epitaxially on α-form crystals [40], and it was reported that the occurrence of γ-form was mainly associated with highly molecular orientation and high pressure [19], and lower the supercooling, higher is the amount of the γ-form crystals produced at a specific pressure [41,42]. In this case, the appearance of γ-form crystals can be attributed to a combination of the local high pressure and shear caused by movement of the pistons and relative high crystallization due to the heterogeneous nucleation of PET dispersed phase. Moreover, for the SCORIM iPP sample, only the skin layer exhibits the γ-form crystals. It appears from experiment that γ-form crystals can grow successfully in this oriented iPP melt with the synergistic effect of shear and pressure only when the growth of β crystals can be restrained by some factors, such as the PET dispersed phase and thermal conditions (cooling rate). Further work is needed and it will be carried out in the near future to challenge this interpretation.

5. Conclusions

The effect of shear stress and PET dispersed phase with various shape on superstructure and distributions (i.e. lamellar orientation and its distribution, lamellar dimension and its distribution, crystalline structure and its distribution) of microfibrillar blend injection molded parts were investigated using SAXS and WAXS. Several conclusions could be drawn from the experimental results of this work.

(1) For the CIM, oriented lamellae (kebabs induced by shish) along the flow direction form in the skin layer, whereas the most lamellae grow radially and form spherulites in the core region; the shear induced crystallization can take place at higher temperature and form a more "stretched" shish-kebab structure which leads to the increase of long spacing of iPP; the β crystals are easy to grow in the intermediate layer because the level of shear rate can induce some row nuclei (shish) and the thermal condition is proper.

When the reciprocating shear rate has imposed on the iPP melt, a more "stretched" shish-kebab structure could also appear in the interior region of moldings which results in the distinct increase of degree of lamellar orientation in this region (i.e. intermediate layer and core region) and the increase of long spacing of iPP; since the shear rate has enhanced by SCORIM even in core region of moldings, the row nuclei can form and induce the formation of β crystals in core region.

(2) For CIM, the distribution of the oriented lamellar crystals (kebabs) can be affected by the addition of different shape of PET dispersed phase. The addition of microfibrils manufactured by the processing with low aspect ratio can lead to distinctly increase the range of kebabs distribution. For the SCORIM, the dynamic shear force becomes dominated factor and the effect of dispersed phase shape can be negligible. Therefore, the degrees of lamellar orientation in the three locations of all the samples have little difference. The heterogeneous nucleation of PET dispersed phase cannot lead to the increase of long spacing as observed in interior region of CIM samples; however, the addition of PET dispersed phase can weaken the shear rate under the same pressure as neat iPP. This results in some decrease of long spacing of iPP especially in interior region of the SCORIM samples. The heterogeneous nucleation of PET dispersed phase can hamper the growth of β crystals; on the other hand, the growth of γ-form crystals takes place in three layers when dynamic shear forces are imposed on the melt. However, it is hard to obtain the γ-form crystals through CIM.

Acknowledgements

The authors gratefully acknowledge the financial support of this subject by National Natural Science Foundation of China (contract nos. 50527301 and 50503015) and Programs for Innovative Research Team in University (JH2005425113461).

We would like to thank Dr. Dmytro Byelov (AMOLF) for SAXS measurements. We are also greatly indebted to Mr. Zhu Li from Analytical and Testing Center of Sichuan University for careful SEM observation.

References

[1] Pantani R, Coccorullo I, Speranza V, Titomanilio G. Prog Polym Sci 2005;30:1185.
[2] Menges G, Wubken G, Horn B. Colloid Polym Sci 1976;254:267.
[3] Viana JC. Polymer 2004;45:993.
[4] Mendoza R, Régnier G, Seiler W, Lebrun JL. Polymer 2003;44:3363.
[5] Kim KH, Isayev AI, Kwon K. J Appl Polym Sci 2005;95:502.
[6] Viana JC, Alves NM, Mano JF. Polym Eng Sci 2004;44:2174.
[7] Guo X, Isayev AI, Guo L. Polym Eng Sci 1999;39:2096.
[8] Warner TJ, Stobbs WM. Acta Metall 1989;37:2873.
[9] Dyer SRA, Lord D, Hutchinson IJ, Ward IM, Duckett RA. J Phys D 1992;25:66.
[10] Sayers CM. Int J Solids Struct 1992;29:2933.
[11] Fu SY, Lauke B. Compos Sci Technol 1996;56:1179.
[12] Fu SY, Lauke B. Compos Sci Technol 1998;58:389.
[13] Choy CL, Leung WP, Kowk KW, Lau FP. Polym Compos 1992;13:69.
[14] Li ZM, Yang MB, Xie BH, Feng JM, Huang R. Polym Eng Sci 2003;43:615.
[15] Li ZM, Yang W, Xie BH, Huang R, Yang MB. Macromol Mater Eng 2004;289:349.
[16] Li ZM, Yang W, Li LB, Xie BH, Huang R, Yang MB. J Polym Sci Polym Phys 2004;42:374.
[17] Li ZM, Li LB, Shen KZ, Yang MB, Huang R. J Polym Sci Polym Phys 2004;42:4095.
[18] Chen LM, Shen KZ. J Appl Polym Sci 2000;78:1906.
[19] Kalay G, Zhong ZP, Allan P, Bevis MJ. Polymer 1996;37:2077.
[20] Zhong GJ, Li LB, Mendes E, Byelov D, Fu Q, Li ZM. Macromolecules 2006;39:6771.
[21] Guan Q, Shen KZ, Ji JL, Zhu JM. J Appl Polym Sci 1995;55:1797.
[22] Mano JF, Sousa RA, Reis RL, Cunha AM, Bevis MJ. Polymer 2001;42:6187.
[23] Li ZM, Yang MB, Feng JM, Huang R. Mater Lett 2002;56:756.
[24] Li LB, Jeu WHD. Macromolecules 2003;36:4862.
[25] Fujiyama M, Wakino T. J Appl Polym Sci 1988;35:29.
[26] Picken SJ, Aerts J, Visser R, Northolt MG. Macromolecules 1990;23:3849.
[27] Turner-Hones A, Cobbold AJ. Polym Lett 1968;6:539.
[28] Zhu PW, Tung J, Phillips A, Edward G. Macromolecules 2006;39:1821.
[29] Lotz B, Wittmann JC, Lovinger AJ. Polymer 1996;37:4979.
[30] Meille SV, Brückner S, Porzio W. Macromolecules 1990;23:4114.
[31] Kumaraswamy G, Issaian AM, Kornfield JA. Macromolecules 1999;32:7537.
[32] Li ZM, Li LB, Shen KZ, Yang W, Huang R, Yang MB. Polymer 2005;46:5358.
[33] Somani RH, Ling Y, Hsiao BS, Sun T, Pogodina NV, Lustiger A. Macromolecules 2005;38:1244.
[34] Varge J, Karger-kocsis J. J Polym Sci Polym Phys 1996;34:657.
[35] Somani RH, Hsiao BS, Nogales A, Fruitwala H, Srinivas S, Tsou AH. Macromolecules 2001;34:5902.
[36] Li ZM, Li LB, Shen KZ, Yang W, Huang R, Yang MB. Macromol Rapid Commun 2004;25:553.
[37] Xu HS, Li ZM, Pan JL, Yang MB, Huang R. Macromol Mater Eng 2004;289:1087.
[38] Smith DE, Babcock HP, Chu S. Science 1999;283:1724.
[39] Saujanya C, Radhakrishnan S. Polymer 2001;42:4537.
[40] Lotz B, Graff S, Straupé C, Wittmann JC. Polymer 1991;32:2902.
[41] Binsbergen FL, Lange BGM. Polymer 1968;9:23.
[42] Campbell RA, Phillips PJ, Lin JS. Polymer 1993;34:4809.